Intersubband magnetophonon resonances in quantum cascade structures

D. Smirnov,* O. Drachenko, and J. Leotin
Laboratoire National des Champs Magnétiques Pulsés, 135 Avenue de Rangueil, 31077 Toulouse, France

H. Page, C. Becker, and C. Sirtori
Laboratoire Central de Recherches Thalès, 91404 Orsay, France

V. Apalkov† and T. Chakraborty‡
Max-Plank-Institut für Physik komplexer Systeme, 01187 Dresden, Germany
(Received 19 April 2002; published 27 September 2002)

We have studied magnetotransport in GaAs/GaAlAs quantum cascade structures. These systems initially designed for intersubband laser emission are peculiar double barrier resonant tunneling structures. Under strong magnetic field applied parallel to the vertical current, we have observed marked quantum oscillations in the magnetoresistance that have field positions independent of the applied bias. These oscillations are explained as intersubband magnetophonon resonance due to electron relaxation by emission of optical phonons.

DOI: 10.1103/PhysRevB.66.125317 PACS number(s): 73.43.Qt, 42.55.Px, 73.21.Fg, 85.35.Be

Ever since the pioneering work by Firsov *et al.*[1] the magnetophonon effect has been regarded as an important tool for investigation of the electron-optical-phonon interaction in semiconductor systems, particularly in confined structures. In a two-dimensional (2D) electron gas under a perpendicular magnetic field, the effect is observed for in-plane transport ($\vec{I}\perp\vec{B}$) of electrons distributed at thermal equilibrium.[2] Quantization of the carrier motion into discrete Landau levels (LLs) of energies $(N+1/2)\hbar\omega_C$, where $\omega_C=eB/m^*$ is the cyclotron frequency, gives rise to quantum oscillations due to resonant *absorption* of longitudinal-optical (LO) phonons that are thermally excited. The magnetophonon resonance (MPR) condition reads $N\hbar\omega_C=\hbar\omega_{LO}$, where N is an integer. The resonant magnetic fields B_N are given by the equation

$$B_N=\frac{1}{N}\frac{m^*}{e}\omega_{LO}.$$

Another situation is met in a quantum well (QW) when the electron distribution between two subbands is strongly out of equilibrium, and the intersubband energy exceeds the LO-phonon energy, $E_2-E_1>\hbar\omega_{LO}$. At high magnetic fields, the energy relaxation into the lower subband takes place in a zero-dimensional system with discrete LLs density of states. The relaxation is inhibited each time energy and momentum conservation forbids transitions mediated by a single phonon.[3–5] In contrast, the relaxation is enhanced when *emission* of a single LO-phonon allows an electron to relax from the upper subband ground LL $E_{2,0}$ into one of the LLs $E_{1,N}$ of the lower subband. This process describes the intersubband MPR resonance given by the equation, $E_{2,0}-E_{1,N}=\hbar\omega_{LO}$. The resonant magnetic fields are expressed by the equation,

$$B_N=\frac{1}{N}\frac{m^*}{e}\left(\frac{E_{2,0}-E_{1,0}}{\hbar}-\omega_{LO}\right). \tag{1}$$

In this paper we report on the observation of the intersubband MPR in the magnetotunneling current ($\vec{I}\|\vec{B}$) in GaAs/GaAlAs quantum cascade lasers (QCL), a device initially designed for mid-infrared emission.[6,7] These systems are a peculiar type of unipolar double barrier resonant tunneling structures (DBRTS).

So far, observation of the intersubband MPR effect has been reported in a bipolar process occurring in the electroluminescence of a GaAs/GaAlAs DBRTS inserted in a *p-i-n* junction.[8] The MPR effect appeared as magneto-oscillations in the luminescence intensity arising from the recombination of electrons and holes in the confined states of the central QW. However, MPR oscillations were not observed clearly in the current across the *p-i-n* junction.

In standard DBRTS what is usually observed in vertical transport ($I\|B$) is (quasi-)elastic or inelastic LO-phonon assisted resonant tunneling across the emitter barrier into the central QW. Typically, in the case of a (quasi)2D emitter biased at a fixed bias V, transitions into the LLs in the well-give current peaks series moving up in magnetic field position as the DBRTS bias is increased.[9,10] In a simple model, the resonance fields depend upon the bias V as

$$B_N(V)=\frac{1}{N}\frac{m^*}{e}\left(\frac{E_0^{inj}+eV-E_{1,0}}{\hbar}-\alpha\omega_{LO}\right), \tag{2}$$

where E_0^{inj} is the emitter level at zero bias, $\alpha=0$ for (quasi-)elastic transitions and $\alpha=1$ for transitions with LO-phonon emission. In addition, inter-LL-tunneling with the emission of two LO phonons ($\alpha=2$) have been observed in a GaAs-AlAs superlattice.[11] By contrast, the MPR peaks positions do not depend on the bias, being only related to the central QWs states. A possible reason for not observing the effect previously in standard DBRTS systems is because the electrons injected into the upper subband can too easily escape from the central well.

Figure 1 shows schematically the measured DBRTS structure with a central region including a three-coupled-QW developing three subbands. The intersubband MPR transitions between E_1 and E_2 subbands are indicated by wavy arrows. The structure includes superlattice emitter-collector regions

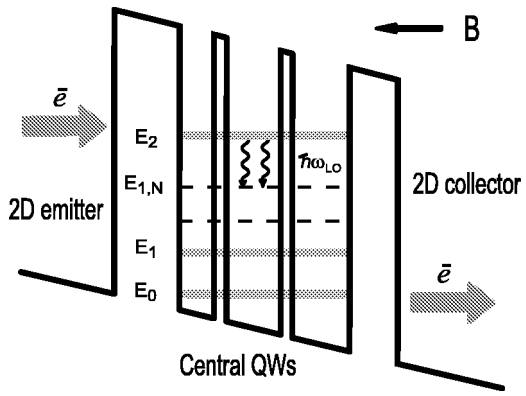

FIG. 1. Conduction band-diagram representing a one period of the laser active region consisting of a double barrier structure. The horizontal arrows symbolize the flow of electrons that are resonantly injected under bias into the central well upper subband E_2. The intersubband magnetophonon resonance is sketched by wavy lines pointing scattering with LO-phonon emission from the ground Landau level of the upper subband $E_{2,0}$ into the excited Landau level $E_{1,N}$ of the lower subband. The E_0 subband is set to accelerate the extraction of electrons toward the collector.

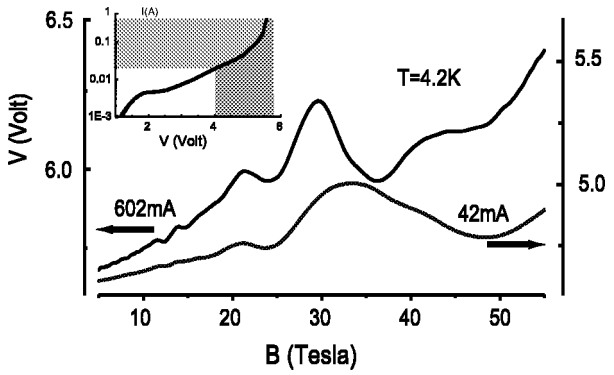

FIG. 2. Voltage across the entire device as a function of magnetic field for two different currents (42 mA and 602 mA) and at 4.2 K. The insert shows the current-voltage curve of the structure at zero magnetic field. The gray area displays the bias range of the magnetotransport measurements.

that are designed as Bragg reflectors to prevent electrons to escape from the upper subband E_2 of the central QW, while allowing their rapid extraction from the lower subband E_0. Another feature of this system is the energy difference between the two lower subbands that matches the LO-phonon energy in order to ensure a rapid extraction of electrons into the collector. Therefore, when the structure is biased to inject electrons into the upper subband, the net result is the inversion of population between E_1 and E_2 subbands. In this situation, the current across the DBRTS becomes controlled by the intersubband relaxation rate since both injection and collection tunneling rates across the barriers are much faster processes. The current then simply reads $I=en/\tau_2$, where n is the electron population and τ_2 the upper subband lifetime. This expression predicts that when the current is set constant, the central well population n must follow the change of the relaxation time with the magnetic field. Then, a peak in the relaxation rate τ_2^{-1}, which occurs at intersubband MPR cause a dip in the central well population. The dip stores a positive charge in the central well while a negative charge is stored in the adjacent collector. The stored charges induce an electric field opposite to the bias field and therefore, produce a series of voltage minima as the magnetic field is swept. Notice that the cascade structure provides a gain on the peak voltage amplitude equal to the number of cascades. On the other hand, when the voltage is set constant the MPR peaks are displayed not by minima but by maxima because the opening of the MPR channels drives more current across the structure.

We measured two sets of GaAs/GaAlAs QCL samples emitting at 11.4 and 9.2 μm wavelength which are described in details in references.[12–14] Since both structures give similar results, we report the data obtained on the 11.4 μ m structure. This sample based on $GaAs/Al_{0.33}Ga_{0.67}As$ heterostructure includes 40 periods between $n+$ doped GaAs ohmic contact layers. The active regions are undoped and consist of 5.6 nm AlGaAs emitter barrier, three coupled GaAs QWs (1.9 nm, 5.8 nm, 4.9 nm width) and 2.8 nm AlGaAs collector barrier. The emitter-collectors are n doped in their central part to obtain under high biases a stable uniform electric field distribution along the entire structure electrically neutral. The structures were processed into mesa-etched bars, 20 μm wide and 1 mm long. The intersubband energies were accurately determined at 4.2 K from spectral luminescence measurements, $E_2-E_1=111$ meV and $E_2-E_0=148$ meV.

Magnetotransport measurements were performed using a pulsed magnet delivering up to 62 T with total pulse duration of 120 ms.[15] All data were obtained at 4.2 K under constant current bias in a wide range from 40 to 600 mA and in the longitudinal configuration $\vec{I}\|\vec{B}$. Short current pulses of 2 μs length and 200 μs repetition time were used in order to avoid heating effects.

We need to identify the bias range where the electrons are effectively injected into the upper subband. Figure 2 displays in the insert the $I(V)$ curve measured at 4.2 K and zero magnetic field. A plateau-like region at about 2 V consists of multiple small negative differential segments, the number of jumps is close to the number of periods of the QCL. Such a structure is caused by sequential alignment of QCL periods.[16] The upper edge of the plateau corresponds to the situation when the 2D-emitter and E_1 states become aligned over all the structure. Above the plateau, the current starts to flow through the upper subband E_2 and reaches the laser threshold at the bias of 6.5 V.

Figure 2 shows the voltage directly measured across the structure as a function of magnetic field for two current biases at 42 mA (4.6 V) and 602 mA (5.7 V). A complex spectrum of oscillations is observed in both curves in the entire field range. A more detailed investigation of the oscillations pattern is obtained by plotting the second derivative $-d^2V/dB^2$. Figure 3(b) presents the results for current biases set respectively, at 42, 50, 100, 314, and 602 mA. The remarkable result is that most of the peaks do not shift in magnetic field position, although the zero-field voltage bias

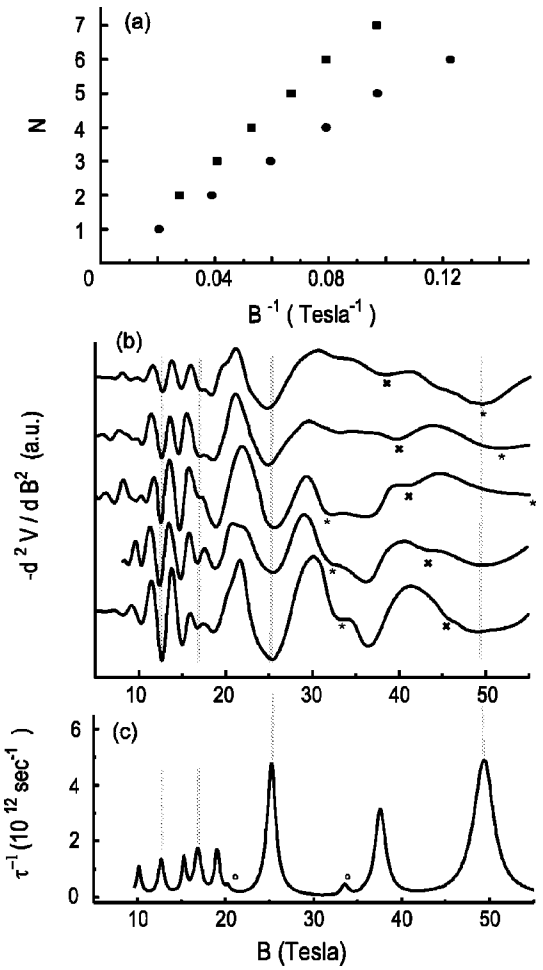

FIG. 3. (a) Fan chart of integers N versus B^{-1} for the current $I=602$ mA. Voltage minima are distributed over two series with fundamental fields ≈ 50 T (circles) and ≈ 74 T (squares). (b) Second derivative of the voltage across the device as a function of the applied magnetic field, at different current bias, respectively from top to bottom, 42, 50, 100, 314, and 602 mA. Most of the oscillations peaks do not shift in magnetic field position as the bias is raised. Vertical lines indicate the series with the fundamental field ≈ 50 T. The asterisks and crosses point the field positions of inelastic LO-phonon assisted tunneling and elastic tunneling. These peaks are not reported in Fig. 3(a). (c) LO-phonon emission rate calculated as a function of applied magnetic field ($B>10$ T) for transitions from the ground Landau level of the upper subband $E_{2,0}$ into the two sets of Landau ladders of lower subbands. Vertical lines correspond to the transitions into $E_{1,N}$. The circles mark the peaks due to acoustic phonons.

is raised by 25%. On the other hand, in the same bias range, a few peaks do shift to higher magnetic fields.

We now analyze the main set of oscillations independent on bias. Figure 3(a) displays a plot of integers versus reciprocal of resonance fields pointed as voltage minima. The two series that appear fulfill the intersubband MPR equation (1). In particular, this model identifies the respective minima at (49.8 ± 0.3)T and (36.8 ± 0.3)T as resonant relaxation from $E_{2,0}$ into $E_{1,1}$ and $E_{0,2}$ LLs. For these values of fields, the cyclotron mass ratios given by Eq. (1) are respectively, (0.0780 ± 0.0005) and (0.0769 ± 0.0006).

To our knowledge there has been no cyclotron resonance measurements of effective masses in GaAs (neither 2D nor bulk) in the range 22–70 T (see, for example, Ref. 17, 18 and reference therein), probably due to the lack of convenient excitation sources. It is thus instructive to compare our results with theoretical calculations. Nonparabolicity effects in a QW in a perpendicular magnetic field have been treated in Ref. 19. We used the approximate analytic expression for the LLs:

$$E_{s,n}(B)=E_s+(N+1/2)\frac{\hbar eB}{m_\parallel}-\frac{1}{8}[(8N^2+8N+1)\alpha' + (N^2+8N+1)\beta']\left[\frac{\hbar eB}{m_b}\right]^2, \quad (3)$$

where $N=0,1,2,\ldots$ is Landau level index, E_s is the subband energy, $m_\parallel=0.069m_0$ is the mass ratio parallel to the layers, $m_b=0.0665m_0$ is the bulk GaAs mass, $\alpha'=0.642$ eV^{-1} and $\beta'=0.697$ eV^{-1}. This model predicts that the cyclotron mass measured at resonance field of 49.8 T should be equal to $0.0795m_0$. The good agreement with our experimental result $(0.0780\pm 0.0005)m_0$ indicates that polaron effects not included in the model are small at such high magnetic fields.

It is of interest to notice that confined phonon modes in the QW do not appear as MPR series. The situation can be completely different in heterostructures with larger dielectric constant difference as AlAs/GaAs.

We briefly analyze the series in Fig. 3(b) which shift with the bias. Equation (2) suggests to plot peak energies per period (eV/40) versus resonant magnetic fields. One finds a quasilinear dependence. The peaks denoted by asterisks have slopes equal to 1.60 and 3.50 meV/T while the peaks pointed by crosses has a slope of 3.3 meV/T. The former peaks are identified as LO-phonon assisted tunneling into $N=2$ and $N=1$ LLs of the QW subband. The latter peaks are interpreted as elastic tunneling transition into the $N=2$ LL of the E_0 QW ground subband.

We finally develop a calculation of the phonons emission rate by electrons in the upper subband ground LL $E_{2.0}$. In addition to LO-phonon, we also include acoustic phonons emission in order to estimate the contribution of this quasielastic intersubband process. The relaxation rate is expressed by the relation

$$\tau_{\mu,i}^{-1}=\frac{2\pi}{\hbar}\sum_j\int\frac{d\vec{Q}}{(2\pi)^3}\delta[\Delta-\hbar\omega_\mu(Q)][1+n_{\mu j}(\vec{Q})] \times|M_{\mu,j}(\vec{Q})Z_i(q_z)|^2R_{0N}(q), \quad (4)$$

where index μ stands for optical (LO) or acoustic (A) phonons, $n_{\mu j}(\vec{Q})$ is the phonon distribution function, $\vec{Q}=(\vec{q},q_z)$ is the three-dimensional vector, j labels the phonon mode, $\omega_{LO}(Q)=\omega_{LO}$ and $\omega_A(Q)=sQ$. $M_{\mu j}(\vec{Q})$ are the matrix elements of electron-phonon interaction.[3,20] For the acoustic phonons we took into account both deformation potential and piezoelectric couplings. The form factors $Z(q_z)$ and $R_{0N}(q)$ are given by the expressions

$$Z_i(q_z) = \int dz e^{iq_z z} \chi_3(z) \chi_i(z),$$

$$R_{0N}(q) = \frac{1}{N!} \frac{(ql_c)^{2N}}{2^N} e^{-(ql_c)^2/2}. \quad (5)$$

To take into account the disorder effect, we introduce the broadening of Landau levels in a Lorentz form with width of 2 meV and average the relaxation rate over Landau level distribution.

Figure 3(c) plots the electron relaxation rate from the E_2 subband into the $N=1-5$ LLs of the lower E_1 and E_0 subbands due to emission of both optical and acoustic phonons. The plot as a function of magnetic field displays the acoustic series mostly in coincidence with optics peaks except at 33.6 T and 20.4 T where weak peaks are visible. The acoustic emission process involves a single phonon of energy less than 1 meV having a wave number $q < l_c^{-1}$ as indicated by the form factor in Eq. (5). In total, the model predicts the overall observed resonance magnetic field positions very well. For example, the optical-phonon emission series agree within 1%(3%) with the data for the series related to the MPR relaxation into the $E_1(E_0)$ subband LLs excited states. We believe the acoustic phonons is at the origin of the weak peaks found in the two measured laser structures.

We finally mention that very recently we obtained another direct signature of the intersubband MPR by measuring the QCL light emission when the device is biased above the laser threshold. At MPR fields, the laser switches off because of the resonant drop of the upper subband population. A detailed analysis of the optical results will be reported in Ref. 21.

In summary, we report a direct evidence of intersubband magnetophonon resonance obtained measuring the magnetoresistance of a double barrier-like structure implemented in a GaAs/GaAlAs quantum cascade laser structure. The effect is manifested as series of magnetoresistance oscillation minima with field positions independent on applied bias. The intersubband MPR provides another spectroscopic tool to investigate the electron-phonon coupling in semiconductor heterostructures.

ACKNOWLEDGMENTS

We wish to acknowledge helpful discussions with B.D. McCombe. We also acknowledge the cooperation of J. Galibert, R. Barbaste and C. Duprat.

*Also at Ioffe Physico-Technical Institute, 194021, Saint Petersburg, Russia.

†Department of Physics, University of Utah, Salt Lake City, Utah 84112.

‡Present address: Institute of Mathematical Sciences, Chennai 600113, India

[1] Yu. A. Firsov, V. L. Gurevich, R. V. Parfeniev, and I. M. Tsidil'kovskii, in *Landau Level Spectroscopy*, edited by G. Landwehr and E. I. Rashba (Elsevier, Amsterdam, 1991), p. 1192; R. J. Nicholas, *ibid.*, p. 779.

[2] D.C. Tsui, Th. Englert, A.Y. Cho, and A.C. Gossard, Phys. Rev. Lett. **44**, 341 (1980).

[3] U. Bockelmann and G. Bastard, Phys. Rev. B **42**, 8947 (1990).

[4] H. Benisty, C.M. Sotomayor-Torres, and C. Weisbuch, Phys. Rev. B **44**, 10 945 (1991).

[5] J. Urayama, *et al.*, Phys. Rev. Lett. **86**, 4930 (2001).

[6] J. Faist, *et al.*, Science **264**, 553 (1994).

[7] J. Faist, *et al.*, Phys. Rev. Lett. **76**, 411 (1996).

[8] P.D. Buckle, J.W. Cockburn, M.S. Skolnick, R. Grey, G. Hill, and M.A. Pate, Phys. Rev. B **53**, 13 651 (1996).

[9] M.L. Leadbeater, E.S. Alves, L. Eaves, M. Henini, O.H. Hughes, A. Celeste, J.C. Portal, G. Hill, and M.A. Pate, Phys. Rev. B **39**, 3438 (1989).

[10] G.S. Boebinger, A.F.J. Levi, S. Schmitt-Rink, A. Passner, L.N. Pfeiffer, and K.W. West, Phys. Rev. Lett. **65**, 235 (1990).

[11] W. Müller, H.T. Grahn, R.J. Haug, and K. Ploog, Phys. Rev. B **46**, 9800 (1992).

[12] C. Sirtori, P. Kruck, S. Barbieri, P. Collot, J. Nagle, M. Beck, J. Faist, and U. Oesterle, Appl. Phys. Lett. **73**, 3486 (1998).

[13] P. Kruck, H. Page, C. Sirtori, S. Barbieri, M. Stellmacher, and J. Nagle, Appl. Phys. Lett. **76**, 3340 (2000).

[14] H. Page, C. Becker, A. Robertson, G. Glastre, V. Ortiz, and C. Sirtori, Appl. Phys. Lett. **78**, 3529 (2001).

[15] O. Portugal, F. Lecouturier, J. Marquez, D. Givord, and S. Askenazy, Physica B **294-295**, 579 (2001).

[16] H.T. Grahn, R.J. Haug, and W. Müller, and K. Ploog, Phys. Rev. Lett. **67**, 1618 (1991).

[17] S.P. Najda, S. Takeyama, N. Miura, P. Pfeffer, and W. Zawadzki, Phys. Rev. B **40**, 6189 (1989).

[18] S. Huant, A. Mandray, and B. Etienne, Phys. Rev. B **46**, 2613 (1992)

[19] U. Ekenberg, Phys. Rev. B **40**, 7714 (1989)

[20] V. F. Gantmakher and Y. B. Levinson, *Carrier Scattering in Metals and Semiconductors* (North-Holland, Amsterdam, 1987); K.A. Benedict, R.K. Hills, and C.J. Mellor, Phys. Rev. B **60**, 10 984 (1999); N. Mori and T. Ando, *ibid.* **40**, 6175 (1989).

[21] D. Smirnov, C. Becker, O. Drachenko, V. Rylkov, H. Page, J. Leotin, and C. Sirtori (unpublished).